Epithelial-mesenchymal transition is necessary for acquired resistance to cisplatin and increases the metastatic potential of nasopharyngeal carcinoma cells

PEI ZHANG[1], HAO LIU[1*], FEI XIA[1], QIAN WEN ZHANG[1], YUAN YUAN ZHANG[1], QING ZHAO[1], ZHEN HUA CHAO[1], ZHI WEN JIANG[1] and CHEN CHEN JIANG[1,2*]

[1]Faculty of Pharmacy, Bengbu Medical College, Anhui Engineering Technology Research Center of Biochemical Pharmaceuticals, Bengbu, Anhui 233030, P.R. China; [2]Priority Research Center for Cancer Research, University of Newcastle, Newcastle, NSW 2308, Australia

Received August 2, 2013; Accepted October 18, 2013

DOI: 10.3892/ijmm.2013.1538

Abstract. Radiotherapy and adjuvant cisplatin (DDP) chemotherapy are standard approaches used in the treatment of nasopharyngeal carcinoma (NPC). However, resistance to chemotherapy has recently become more common, resulting in the failure of this combination therapy for NPC. The aim of the present study was to assess the cellular morphology, motility and molecular changes in DDP-resistant NPC cells in relation to epithelial-mesenchymal transition (EMT). CNE2 cells were continuously exposed to increasing doses of DDP to establish a stable cell line resistant to DDP (CNE2/DDP cells). The human NPC cell lines, HNE1, CNE2, HNE1/DDP and CNE2/DDP, were used to examine the association between chemoresistance and the acquisition of an EMT-like phenotype of cancer cells. The DDP-resistant cells were less sensitive than the HNE1 cells to treatment with DDP, and were shown by a cell viability assay, western blot analysis and qRT-PCR to have acquired chemoresistance. The HNE1/DDP cells examined by wound healing and Transwell Boyden chamber assays exhibited an increased migration and invasion potential. The DDP-resistant cells exhibited morphological and molecular changes consistent with EMT, as observed by western blot analysis and qRT-PCR. These changes included becoming more spindle-like in shape, a loss of polarity and formation of pseudopodia, the downregulation of E-cadherin and β-catenin and the upregulation of vimentin, fibronectin and matrix metalloproteinase (MMP)-9. Moreover, the levels of the EMT-related transcription factors, Snail, Slug, Twist and zinc finger E-box binding homeobox 1 (ZEB1), were higher in the DDP-resistant NPC cells. These data suggest that the development of DDP resistance of NPC cells is accompanied by inducible EMT-like changes with an increased metastatic potential *in vitro*. Further elucidation of the association between resistance to DDP and EMT may facilitate the future development of novel therapeutic approaches for the treatment of chemoresistant tumors.

Correspondence to: Professor Hao Liu, Faculty of Pharmacy, Bengbu Medical College, Anhui Engineering Technology Research Center of Biochemical Pharmaceuticals, 2600 Donghai Dadao, Bengbu, Anhui 233030, P.R. China
E-mail: liuhao6886@foxmail.com

Professor Chen Chen Jiang, Priority Research Center for Cancer Research, University of Newcastle, Newcastle, NSW 2308, Australia
E-mail: chenchen_jiang@newcastle.edu.au

*Contributed equally

Key words: nasopharyngeal carcinoma, chemoresistance, invasion, migration, epithelial-mesenchymal transition

Introduction

Nasopharyngeal carcinoma (NPC) is one of the most common types of head and neck cancer in Asia, particularly in Southeast Asia and China, with a high incidence rate of approximately 20-50 cases per 100,000 individuals per year (1). By contrast, NPC is rare in the United States (apart from Alaska) and Western Europe, with an incidence of <1/100,000 individuals. The accurate detection of NPC is not easy due to its anatomical location. In conventional clinical therapy, radiotherapy is the primary therapeutic approach, while using radiotherapy combined with chemotherapy is recommended for the treatment of advanced carcinoma (2). However, the 5-year survival rate is extremely low. Treatment failure rates remain high due to the development of drug resistance and distant metastasis.

Drug resistance is a major complication in cancer chemotherapy. It accounts for the ineffectiveness of chemotherapy in the majority of cancer patients (3). Resistance occurs when tumor cells do not respond to anticancer drugs. Cisplatin (DDP) is clinically used as adjuvant therapy for NPC in order to induce tumor cell death. DDP induces cytotoxicity and/or apoptosis by forming DNA adducts or by targeting proteins/enzymes and pathways (4-6). However, the efficacy of DDP is often accompanied by chemoresistance. The mechanisms through which NPC cells acquire chemoresistance are unknown. Thus, a better understanding of the mechanisms through which cells acquire resistance and knowledge of the molecular alterations which induce or correlate with resistance may lead to the development of novel therapeutic strategies for NPC (7,8).

Recent evidence suggests that epithelial-mesenchymal transition (EMT)-type cells play critical roles in chemoresistance. Thus, the molecular basis of chemoresistance in relation to EMT is currently an important focus of cancer research. EMT describes a series of marked morphological changes, characterized by a transition from an epithelial to a mesenchymal phenotype, leading to increased motility and invasion (9). During the acquisition of EMT characteristics, cells lose epithelial cell-cell junctions and undergo actin cytoskeletal reorganization. The downregulation of epithelial molecular markers, such as E-cadherin and β-catenin is also observed, as well as an upregulation of mesenchymal molecular markers, such as vimentin, fibronectin, α-smooth muscle actin (α-SMA) and N-cadherin. An increase in the production of transcription factors that repress E-cadherin expression, including Twist, zinc finger E-box binding homeobox 1 (ZEB1), Snail and Slug also occurs, as well as an increase in the activity of matrix metalloproteinases (MMPs), such as MMP-2 and MMP-9, associated with an invasive phenotype (10). The process of EMT has also been shown to be important in conferring drug resistance to cancer cells against conventional therapeutics. Several chemotherapeutic drug-resistant cell lines established *in vitro,* such as tamoxifen-resistant breast cancer (11), paclitaxel-resistant ovarian cancer (12), oxaliplatin-resistant colorectal cancer and gemcitabine-resistant pancreatic cancer (13) cell lines have shown phenotypic changes consistent with EMT. These data clearly provide strong evidence for linking chemoresistance to EMT. However, DDP-resistant NPC cells have not been extensively studied.

In the present study, we isolated DDP-resistant cells from well-characterized NPC cell lines and determined that they have numerous EMT-like properties. We demonstrate that DDP-resistant cells are insensitive to DDP and have a strong invasion and migration ability. The characterization of these stable NPC cells may provide new insight into the phenotypic changes associated with resistance to DDP.

Materials and methods

Reagents and antibodies. DDP was purchased from Qilu Pharmaceutical Co., Ltd. (Jinan, China). RPMI-1640 medium, fetal bovine serum (FBS) and phosphate-buffered saline (PBS) were purchased from Gibco-BRL (Grand Island, NY, USA). Matrigel was purchased from BD Biosciences (Bedford, MA, USA). We purchased 3-(4,5-dimethylthiazol-2-yl)-2,5-diphenyltetrazolium bromide (MTT) from Sigma Chemical Co. (Castle Hill, Australia). The antibodies against Bcl-2, Bax, Puma and myeloid cell leukemia-1 (Mcl-1; 1:100) were purchased from Beijing Biosynthesis Biotechnology Co., Ltd. (Beijing, China). Primary antibodies against E-cadherin, β-catenin, vimentin, fibronectin, MMP-9, Twist, Slug, Snail, ZEB1 (1:500) and β-actin (1:2,000) were obtained from Santa Cruz Biotechnology Inc. (Santa Cruz, CA, USA).

Cell lines and culture. The human NPC cell lines, HNE1, HNE1/DDP and CNE2, were obtained from Sun Yat-Sen University (Guangzhou, China) and maintained in our laboratory. The HNE1, HNE1/DDP and CNE2 cells were cultured in RPMI-1640 medium containing 10% FBS, penicillin (100 U/ml) and streptomycin (100 U/ml), in a humidified atmosphere of 5% CO_2 at 37˚C. The RPMI-1640 medium for the HNE1/DDP cells was also supplemented with 4 μmol/l DDP. All cell lines were tested each month for mycoplasma contamination, used only at low passage and regularly examined under a microscope for phenotypic changes prior to use.

Cell growth assay. To investigate cell growth, we performed a cell proliferation assay on cells ($1x10^4$ cells/well) plated in 24-well Costar® plates (Corning Life Sciences, Corning, NY, USA). The experiments were carried out for 168 h, and the number of cells was counted every 24 h. Cells from 3 samples were trypsinized and counted using a hemocytometer at the indicated time points.

Morphological analysis. Cells were grown to 70% confluence in DDP-free medium appropriate for the parental cell lines and in medium with DDP for the DDP-resistant cell lines. They were visualised under a light microscope (CKX41; Olympus, Tokyo, Japan). Digital images were captured using a camera mounted to the microscope (cellSens Entry; Olympus).

Cell viability assay. Cell viability was assessed by MTT assay. MTT is a yellow tetrazolium dye responding to metabolic activity. In living cells, reductase enzymes alter the MTT color from a light yellow to deep blue, corresponding to formazan crystals. Briefly, $7x10^3$ cells/well were plated in 96-well Costar® culture plates in triplicate. Following 24 h of incubation, the cells were treated with various concentrations of DDP and subsequently incubated for 24, 48 and 72 h. At the end of the incubation period, 20 μl MTT were added to achieve a final concentration of 0.5 mg/ml. The cells were then incubated for a further 4 h. The medium and MTT were then removed before 150 μl dimethylsulfoxide (DMSO) was added to each well to dissolve the crystals. The optical density (OD) of the formazan product was determined at a 570 nm wavelength using a microplate reader (Bio-Tek Instruments Inc., Winooski, VT, USA). Cell viability (%) = $(OD_{sample} - OD_{blank})/(OD_{control} - OD_{blank})$ x100. The IC_{50} value, defined as the drug concentration required to reduce cell survival to 50%, was determined by the relative absorbance of MTT. All experiments were performed in triplicate.

Wound healing assay. Cell migration was assessed using a wound healing assay. Cells were plated in 6-well plates (Corning Life Sciences) at $5x10^5$ cells/well and allowed to grow to 90% confluence. The cells were scraped with a sterile micropipette tip to create a gap of standard width. To remove non-adherent cells, the plates were rinsed gently with medium twice prior to incubation. The wound closure was monitored for 24 h at x100 magnification. The wound areas were observed under an inverted microscope and imaged at the appropriate fields to calculate the healing percentages. Each experiment was performed in triplicate.

Invasion and migration assay. The ability of the cells to pass through filters was measured using a Transwell Boyden chamber system (Corning Life Sciences) containing a polycarbonate filter (6.5 mm in diameter, 8 μm pore size). The membrane undersurface was coated with 50 μl of Matrigel, mixed with RPMI-1640 serum-deprived medium at a 1:8 dilu-

tion and subsequently applied to the top side of the filter for the cell invasion assay. By contrast, the filter was not coated for the cell migration assay. The cells were resuspended in serum-deprived medium. Subsequently, 200 μl of the cell suspension ($5x10^4$ cells/well) were added to the upper chamber, while 600 μl RPMI-1640 medium containing 10% FBS were added to the lower chamber and served as a chemoattractant. The system was incubated for 24 h at 37˚C. The cells that did not migrate or invade after 24 h were removed from the upper face of the filters by scrubbing with a cotton swab. The membrane was then fixed with 4% formaldehyde for 15 min at room temperature and stained with 0.5% crystal violet for 15 min. Finally, 5 visual fields were randomly selected from each membrane and photographed under a light microscope at x200 magnification. The number of migrating or invading cells was then counted and analyzed to determine statistically significant differences. Each condition was assayed in triplicate. The experiments were performed independently at least 3 times. The results were expressed as the number of cells per field.

Quantitative reverse transcription PCR (qRT-PCR). Total RNA was isolated using TRIzol reagent (Invitrogen Life Technologies, Carlsbad, CA, USA). Aliquots (1 μg) of RNA were reverse transcribed to cDNA (20 μl) using oligo(dT) and M-MuLV reverse transcriptase (Fermentas Inc., Glen Burnie, MD, USA) following the instructions of the manufacturer. One-fifth of the cDNA was used as a template for PCR using the SYBR®-Green PCR kit (Takara, Kyoto, Japan) in an ABI StepOne™ Real-Time PCR System (Applied Biosystems, Foster City, CA, USA). The housekeeping gene, glyceraldehyde-3-phosphate dehydrogenase (GAPDH), was selected as an internal control for each experiment. The primers used in this study are presented in Table I. The cycling conditions were as follows: pre-denaturation at 95˚C for 10 min, followed by 40 cycles at 95˚C for 10 sec, at 57-60˚C for 20 sec and at 72˚C for 15 sec. The specificity of the amplification products was confirmed by a melting curve analysis. All reactions were run in triplicate. As a measure of relative change in expression between the parental and resistant samples, ΔΔCt values were calculated and converted to approximate fold change values ($2^{-\Delta\Delta Ct}$).

Western blot analysis. The cells were plated in 6-well culture dishes (Corning Life Sciences) at a density of $4x10^5$ cells/well. Following 24 h of incubation, the cells were washed with 1 ml PBS/well and harvested using trypsin. Harvested cells were centrifuged and resuspended in lysis buffer. Following incubation on ice for 30 min, the homogenate was centrifuged at 12,000 rpm for 30 min at 4˚C. Protein concentrations were determined using a bicinchoninic acid (BCA) assay (Beyotime Institute of Biotechnology, Beijing, China). Subsequently, 40 μg of protein were separated using 10-15% sodium dodecyl sulfate-polyacrylamide gel electrophoresis (SDS-PAGE), and transferred onto polyvinylidene difluoride (PVDF) membranes. The blotted membranes were blocked with 5% skim milk for 2 h, and probed with primary antibodies overnight at 4˚C. The membranes were washed and probed with secondary antibodies for 2 h. The membranes were imaged with gel imaging equipment (Bio-Rad, Hercules, CA, USA). β-actin was used as the loading control.

Table I. Primers used for qRT-PCR.

Gene	Primer sequence (5'-3')	Product size (bp)
MDR1	F: CCCATCATTGCAATAGCAGG R: GTTCAAACTTCTGCTCCTGA	157
MRP	F: AGGAGAGATCATCATCGATGG R: GCCTTCTGCACATTCATGG	235
Bcl-2	F: CGACGACTTCTCCCGCCGCTACCGC R: CCGCATGCTGGGGCCGTACAGTTCC	319
Bax	F: TTTGCTTCAGGGTTTCATCC R: CAGTTGAAGTTGCCGTCAGA	246
E-cadherin	F: CATTTCCCAACTCCTCTCCTGGC R: ATGGGCCTTTTTCATTTTCTGGG	90
β-catenin	F: CACAAGCAGAGTGCTGAAGGTG R: GATTCCTGAGAGTCCAAAGACAG	146
Vimentin	F: AGATGGCCCTTGACATTGAG R: TGGAAGAGGCAGAGAAATTC	80
Fibronectin	F: CCCACCGTCTCAACATGCTTAG R: CTCGGCTTCCTCCATAACAAGTAC	264
MMP-9	F: CGGAGTGAGTTGAACCAG R: GTCCCAGTGGGGATTTAC	118
Snail	F: CCAGCTCTCTGAGGCCAAGGATC R: TGGCTTCGGATGTGCATCTTGAG	108
Slug	F: CCCTGAAGATGCATATTCGGAC R: CTTCTCCCCCGTTGTAGTTCTA	116
Twist	F: TGCGGAAGATCATCCCCA R: TCCATCCTCCAGACCGAGAA	187
ZEB1	F: GCACAACCAAGTGCAGAAGA R: GCCTGGTTCAGGAGAAGATG	141
GAPDH	F: AGAAGGCTGGGGCTCATTTG R: AGGGGCCATCCACAGTCTTC	258

F, forward; R, reverse sequence; MDR, multidrug resistance; MRP, multidrug resistance-associated protein; MMP, matrix metalloproteinase; ZEB1, zinc finger E-box binding homeobox 1; GAPDH, glyceraldehyde-3-phosphate dehydrogenase.

Establishment of DDP-resistant NPC cells. The CNE2 cells were thoroughly washed with PBS and transferred to RPMI-1640 medium, containing 10% FBS and penicillin-streptomycin. To create stable NPC cells resistant to DDP, the CNE2 cells were continuously exposed to DDP for >9 months. During this period, the medium was replaced every 3 days and the cell cultures were passaged by trypsinization after 70-80% confluency was reached. Gradually, the cells displayed resistance to the growth-inhibitory properties of DDP. The DDP-resistant CNE2 cells were cultured in medium containing DDP for 3 additional months prior to characterization. Through this process, we generated a stable DDP-resistant cell line (CNE2/DDP cells).

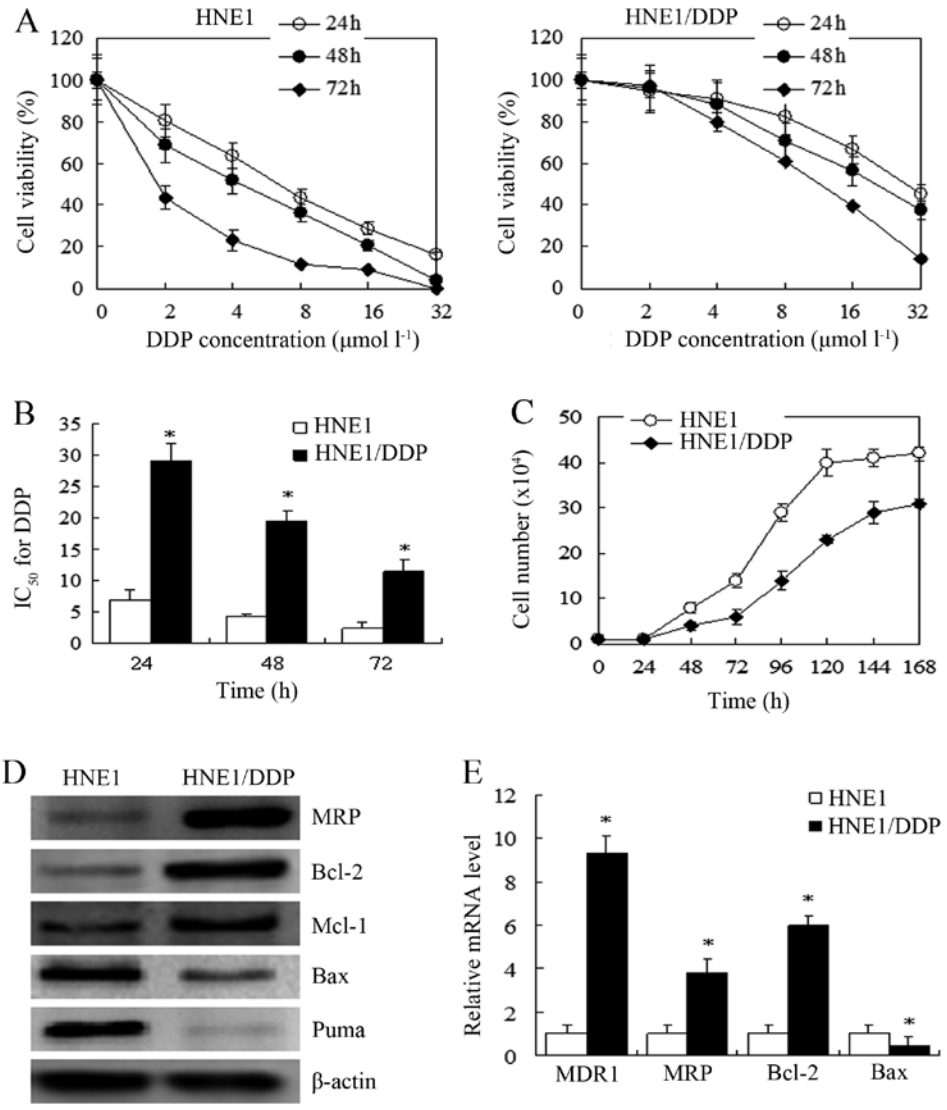

Figure 1. HNE1/DDP cells exhibited chemoresistance to cisplatin (DDP) compared with the parental HNE1 cells. (A) DDP inhibited the growth of nasopharyngeal carcinoma (NPC) cells. HNE1 and HNE1/DDP cells were treated with DDP at various concentrations (2, 4, 8, 16 and 32 μmol/l) for 24, 48 and 72 h, then 3-(4,5-dimethylthiazol-2-yl)-2,5-diphenyltetrazolium bromide (MTT) was added to determine cell viability. Results are expressed as a percentage of control levels. (B) IC_{50} values of HNE1/DDP and HNE1 cells for 24, 48 and 72 h (means ± SEM, n=3, *P<0.05 compared with the parental HNE1 cells). (C) Proliferation of HNE1 and HNE1/DDP cells in the normal culture medium was examined by determination of the cell numbers at different time points after cell seeding at the same number. (D) Expression levels of multidrug resistance-associated protein (MRP), Bcl-2, myeloid cell leukemia-1 (Mcl-1), Bax and Puma proteins in the HNE1 and HNE1/DDP cells were determined by western blot analysis. (E) Relative mRNA expression levels of MDR1, MRP, Bcl-2 and Bax genes in the HNE1 and HNE1/DDP cells were analyzed by qRT-PCR (means ± SEM, n=3, *P<0.05 compared with parental HNE1 cells).

Statistical analysis. All experiments were repeated at least 3 times. Data are presented as the means ± SEM. The differences between mean values were analyzed using the two-tailed Student's t-test. All statistical analyses were performed using SPSS 13.0 software (SPSS Inc., Chicago, IL, USA). P-values <0.05 were considered to indicate statistically significant differences.

Results

HNE1/DDP cells exhibit chemoresistance to DDP. We first confirmed the resistance of NPC cells to DDP by an MTT assay. The proliferation of NPC cells was inhibited by various concentrations of DDP (Fig. 1A). Chemoresistance to DDP was observed in the HNE1/DDP cells, as compared with the HNE1 cells. The inhibitory effects of increasing DDP concentrations on proliferation were more pronounced with HNE1 than with HNE1/DDP cells. The IC_{50} values of HNE1/DDP and HNE1 cells were 29.04±2.82, 19.44±1.77 and 11.39±1.89 μmol/l and 6.84±1.59, 4.25±0.36 and 2.35±0.96 μmol/l for 24, 48 and 72 h, respectively (Fig. 1B). Thus, DDP inhibited the proliferation of the cells. In addition, the HNE1/DDP cells were less sensitive than the HNE1 cells to treatment with DDP. The HNE1/DDP cells proliferated less than the HNE1 cells under normal culture conditions (Fig. 1C). By western blot analysis, we then examined the protein expression levels of multidrug resistance-associated protein (MRP), Mcl-1, Bcl-2, Bax and Puma to further determine the chemoresistance (Fig. 1D). The expression levels of MRP, Mcl-1 and Bcl-2 were higher in the HNE1/DDP cells compared with the HNE1 cells. Additionally,

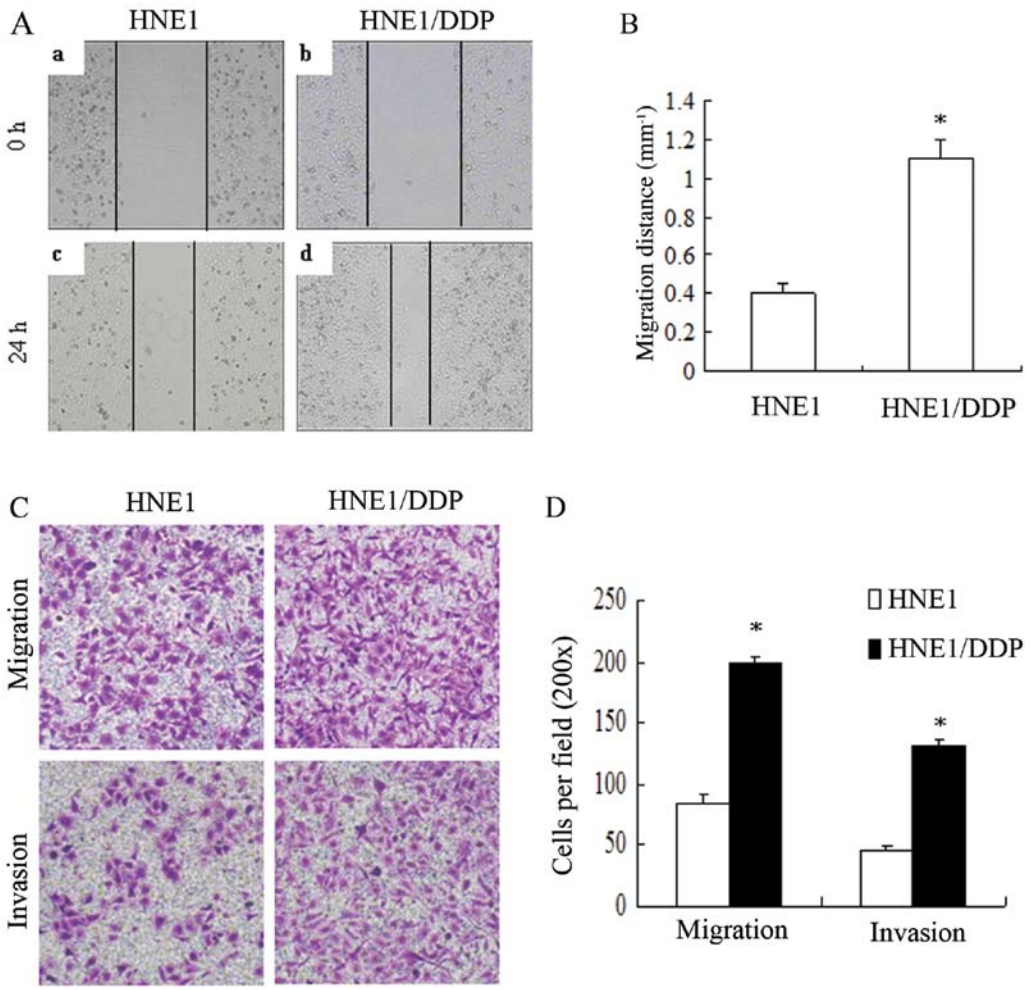

Figure 2. HNE1/DDP cells have increased migration and invasion potential. (A) Wound healing assays were performed to compare the migration potential of HNE1/DDP and parental HNE1 cells at x100 magnification. (A and B) HNE1 and HNE1/DDP cells at time zero. (C and D) HNE1 and HNE1/DDP cells following 24 h of incubation. (B) Quantitative results are expressed as a wound healing index, which was calculated using 5 randomly selected distances across the wound at 0 and 24 h (means ± SEM, n=3, *P<0.05 compared with parental HNE1 cells). (C) Transwell Boyden chamber assays were performed to compare the migration and invasion potential of HNE1/DDP and parental HNE1 cells after 24 h of incubation at x200 magnification. (D) Quantitative results are shown as migrating and invading cells, which were calculated using 5 visual fields selected in the Transwell migration and invasion assays (means ± SEM, n=3, *P<0.05 compared with the parental HNE1 cells).

the expression levels of Bax and Puma were lower in the HNE1/DDP cells. Moreover, the Bcl-2/Bax ratio was lower in the HNE1 cells. qRT-PCR further revealed that multidrug resistance (MDR)1, MRP and Bcl-2 were upregulated and that Bax was downregulated in the HNE1/DDP cells (Fig. 1E). Based on these observations, we concluded that the HNE1/DDP cells had acquired chemoresistance.

HNE1/DDP cells have an increased migration and invasion potential in vitro. We then compared the HNE1/DDP and HNE1 cells for various cellular functions. Since the acquisition of chemoresistance generally correlated with an increased migration and invasion ability in the progression of tumors, we measured the migration and invasion ability of the HNE1/DDP and HNE1 cells using wound healing and Transwell Boyden chamber assays. Wound healing assays were performed to compare the migration potential of the HNE1/DDP and the parental HNE1 cells. At 24 h, a 2.7-fold increase in the number of HNE1/DDP cells migrating across the wound was observed (P<0.05) (Fig. 2A and B). In addition, we compared the migration and invasion potential between the HNE1/DDP and HNE1 cells using Transwell Boyden chamber assays. At 24 h, the HNE1/DDP cells showed a 2.2-fold increase in migration and a 2.8-fold increase in invasion compared with the HNE1 cells (P<0.05) (Fig. 2C and D). Thus, the HNE1/DDP cells had an increased migration and invasion potential as compared with the parental HNE1 cells.

HNE1/DDP cells display morphological and molecular changes consistent with EMT. Cell morphology was examined by microscopy at x200 magnification (Fig. 3A). The parental HNE1 cells showed an epithelioid, cobblestone appearance that was rounded and contained few formations of pseudopodia. By contrast, the phenotypic changes observed in the HNE1/DDP cells included a loss of cell polarity, development of a spindle-shaped morphology and increased formation of pseudopodia. To determine whether the acquisition of resistance to DDP induced specific molecular changes consistent with EMT, western blot analysis and qRT-PCR were performed and revealed that the expression of epithelial markers, such as

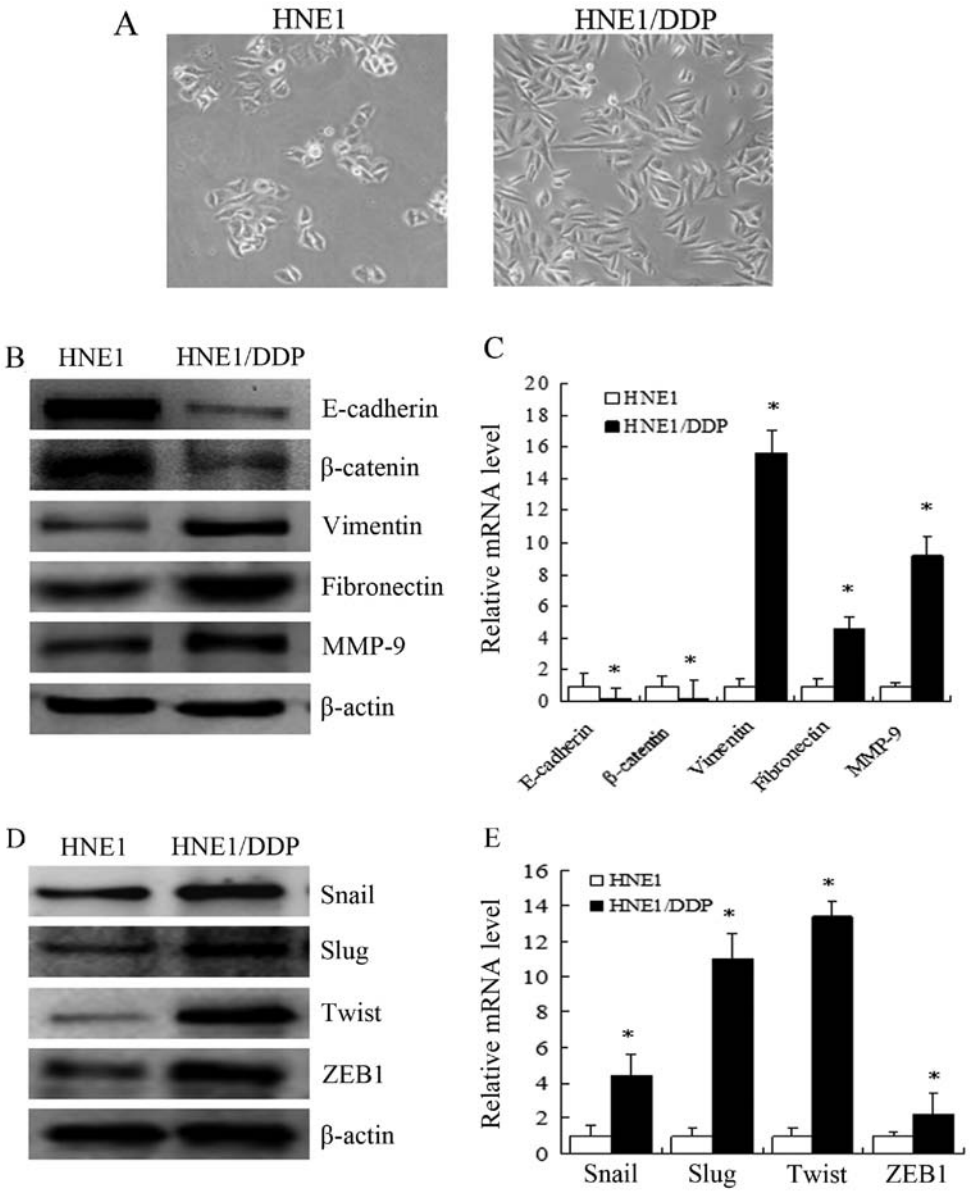

Figure 3. HNE1/DDP cells exhibit morphological and molecular changes consistent with epithelial-mesenchymal transition (EMT). (A) Cell morphology was observed by microscopy at x200 magnification. The parental HNE1 cells showed an epithelioid, cobblestone rounded appearance with limited formation of pseudopodia. By contrast, the phenotypic changes observed in the HNE1/DDP cells included a loss of cell polarity, causing a spindle-shaped morphology and an increased formation of pseudopodia. (B) Expression levels of the EMT-related proteins, E-cadherin, β-catenin, vimentin, fibronectin and matrix metalloproteinase (MMP)-9, were determined by western blot analysis. The downregulation of E-cadherin and β-catenin and upregulation of vimentin, fibronectin and MMP-9 was observed in the HNE1/DDP cells. (C) mRNA expression levels of E-cadherin, β-catenin, vimentin, fibronectin and MMP-9 genes were analyzed by qRT-PCR (means ± SEM, n=3, *P<0.05 compared with the parental HNE1 cells). (D) Increased protein levels of the EMT-related transcription factors, Snail, Slug, Twist and zinc finger E-box binding homeobox 1 (ZEB1), were determined by western blot analysis. (E) mRNA expression levels of the genes coding for the EMT-related transcription factors, Snail, Slug, Twist and ZEB1, were analyzed by qRT-PCR (means ± SEM, n=3, *P<0.05 compared with the parental HNE1 cells).

E-cadherin and β-catenin, was reduced in the HNE1/DDP cells compared with the HNE1 cells. The expression of mesenchymal markers, such as vimentin and fibronectin, was higher in the HNE1/DDP cells (P<0.05) (Fig. 3B and C). Moreover, the mRNA and protein levels of MMP-9 were higher in the HNE1/DDP cells compared with the HNE1 cells (P<0.05) (Fig. 3B and C). Furthermore, the mRNA and protein levels of the EMT-related transcription factors, Snail, Slug, Twist and ZEB1, were higher in the HNE1/DDP cells compared with the HNE1 cells (P<0.05) (Fig. 3D and E). Based on these observations, HNE1/DDP cells were considered to have acquired a mesenchymal phenotype.

CNE2 cells undergo an EMT-like transformation induced by DDP. We further examined whether the occurrence of EMT and the enhanced expression of EMT-related molecules were observed in other NPC cell lines resistant to DDP. For this purpose, we established a stable DDP-resistant NPC cell line (CNE2/DDP cells). The CNE2/DDP cells were less sensitive than the CNE2 cells to treatment with DDP (data not shown). As shown in Fig. 4A, the parental CNE2 cells showed an epithelioid, cobblestone appearance, similar to the HNE1 cells. By contrast, the morphology of the CNE2/DDP cells was mixed: they showed an epithelioid, long, spindle/fibroblastic-like shape, along with formation of pseudopodia

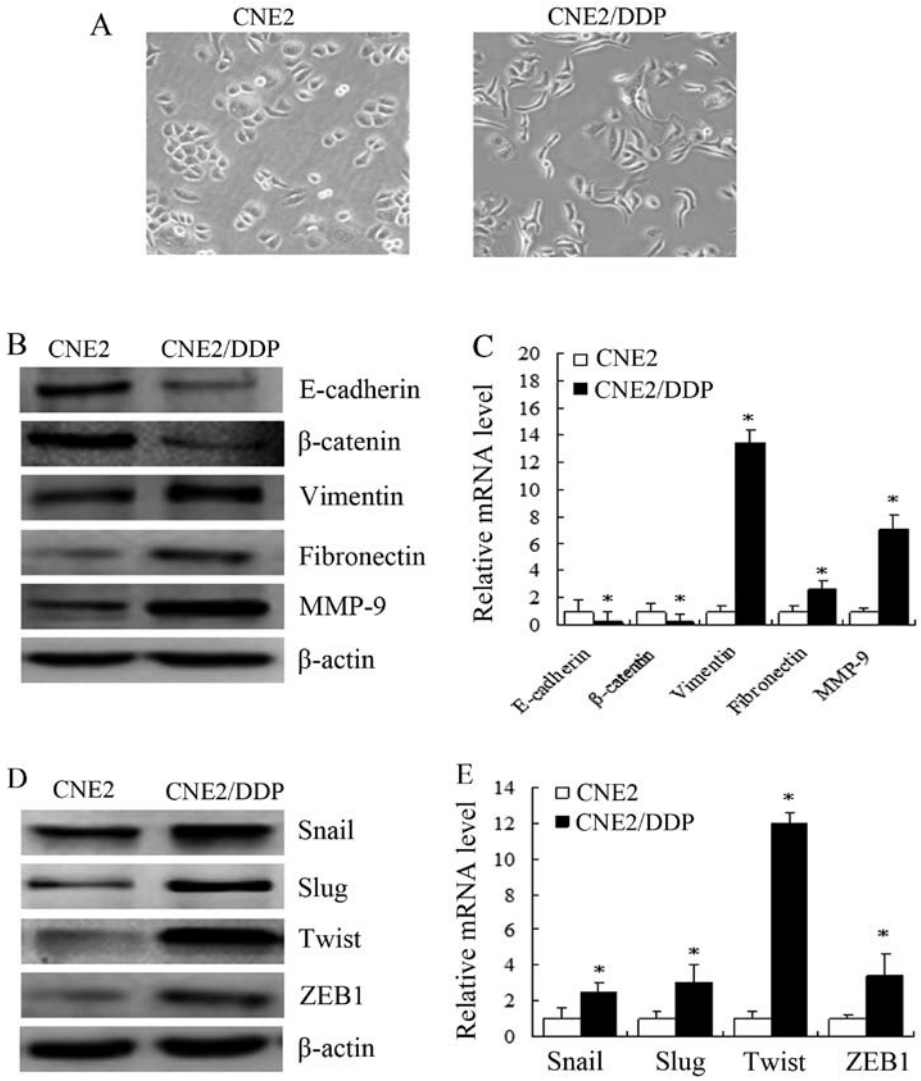

Figure 4. Cisplatin (DDP)-treated CNE2 cells underwent an epithelial-mesenchymal transition (EMT)-like transformation. (A) Cell morphology was observed by microscopy at x200 magnification. Parental CNE2 cells showed an epithelioid, cobblestone appearance, similar to HNE1 cells. By contrast, the morphology of CNE2/DDP cells was of mixed type, showing an epithelioid, long, spindle/fibroblastic pattern with pseudopodia and an unorganized growth pattern. (B) Expression levels of the EMT-related proteins, E-cadherin, β-catenin, vimentin, fibronectin and matrix metalloproteinase (MMP)-9, were determined by western blot analysis. The downregulation of E-cadherin and β-catenin and upregulation of vimentin, fibronectin and MMP-9 was observed in CNE2/DDP cells. (C) mRNA expression levels of E-cadherin, β-catenin, vimentin, fibronectin and MMP-9 genes were analyzed by qRT-PCR (means ± SEM, n=3, *P<0.05 compared with the parental CNE2 cells). (D) Increased protein levels of the EMT-related transcription factors, Snail, Slug, Twist and zinc finger E-box binding homeobox 1 (ZEB1), were determined by western blot analysis. (E) mRNA expression levels for genes coding for the EMT-related transcription factors, Snail, Slug, Twist and ZEB1, were analyzed by qRT-PCR (means ± SEM, n=3, *P<0.05 compared with parental CNE2 cells).

and an unorganized growth pattern. Furthermore, higher levels of mesenchymal markers, such as vimentin, fibronectin and MMP-9, and lower levels of epithelial markers, such as E-cadherin and β-catenin, were observed in the CNE2/DDP cells compared with the parental CNE2 cells (P<0.05) (Fig. 4B and C). In addition, the mRNA and protein levels of the EMT-related transcription factors, Snail, Slug, Twist and ZEB1, were higher in the CNE2/DDP cells compared with the CNE2 cells (P<0.05) (Fig. 4D and E).

Discussion

Chemotherapy with DDP is widely used in the treatment of NPC patients; DDP as the most active and commonly used drug is often applied for the treatment of distant metastasis or advanced locoregional recurrence in NPC patients (14). However, the development of resistance to DDP is a major limitation to its use in cancer chemotherapy (15). The biological mechanisms through which DDP leads to DDP resistance are now beginning to be understood, and have the potential to provide molecular targets for therapeutic intervention, improve the prediction of response and allow the development of strategies to overcome resistance to DDP. To further examine these mechanisms, we selected DDP-resistant NPC cells, HNE1/DDP cells and parental HNE1 cells. Our results revealed that the HNE1/DDP cells have acquired the characteristics of chemoresistance.

Previous studies of chemoresistance and metastasis have been in general separately performed in the cancer research field. Thus, little is known as to the association between chemoresistance and cancer metastasis. Nevertheless, there are two observations of interest: firstly, a number of tumor

cells selected for resistance to drugs have a greater metastatic potential compared with non-resistant parental cells. Secondly, secondary (greater metastatic potential) tumors are more resistant to chemotherapeutic drugs than their primary counterparts in a number of cases (16). Metastasis is a complicated multi-step process which includes local invasion, intravasation, survival during transport through the vasculature, arrest at the capillaries, extravasation and, finally, outgrowth to form macrometastatic tumors in distant organs (17,18). Clinically, an enhanced metastatic ability and chemoresistance are frequently concurrent during the therapeutic course of NPC, and seem to be linked in light of the evolution towards increasingly malignant characteristics in tumors. However, in several cases, no correlation has been observed between chemoresistance and cancer metastasis (19). One study demonstrated that a calcium-resistant human fibrosarcoma HI-1080 Cd-R cell variant was developed, which was cross-resistant to DDP and more invasive than parental HIT-1080 Cd-R cells, as shown by Transwell *in vitro* assays. In addition, an increased expression of MMP-9 has been observed in HT-1080 Cd-R cells (20). In the present study, we demonstrated that the HNE1/DDP cells acquired an increased capacity for migration and invasion *in vitro* during the development of resistance to DDP. Furthermore, the mRNA and protein levels of MMP-9 were increased in the HNE1/DDP cells. Therefore, chemoresistance and metastasis are the main obstacles in the current clinical management of NPC. Preventing, predicting and inhibiting chemoresistance and metastasis in NPC is critical for further improving the survival rate of patients with NPC.

Increasing evidence supports a molecular and phenotypic association between chemoresistance and the acquisition of the EMT-like phenotype in cancer cells. It is well established that epithelial cells can acquire a mesenchymal phenotype through fundamental and complex processes (21). While EMT has been widely studied for its role in early development and cancer metastasis, it can also influence the cellular ability to evade the effects of platinum-based therapies (22). EMT induces the transformation of a differentiated epithelial cell into a mesenchymal cell with stem-like properties, and is characterized by the loss of cell-to-cell adhesion, tight and gap junctions, as well as the loss of cell polarity and increased motility (23). Recent studies have indicated that EMT may enhance the cancer development progress, by showing that the epithelial-derived tumor cells can change into a more preliminary mesenchymal phenotype that facilitates motility and invasion (24,25). In this study, with a series of experiments, we demonstrated that the acquisition of resistance to DDP by NPC cells leads to morphological and molecular alterations consistent with a change to a mesenchymal-like phenotype. We also obtained molecular evidence that the EMT-like changes in the DDP-resistant NPC cell line were associated with an increase in the expression of the transcription factors, Snail, Slug, Twist and ZEB1. These are the major transcription factors responsible for the development of EMT, and bind directly to the E-boxes of the E-cadherin promoter to repress the transcription of this gene (26). However, the expression of Twist in the DDP-resistant NPC cell line was significantly increased at both the mRNA and protein levels. The increased expression of Twist was responsible for the development of acquired resistance to paclitaxel in NPC cells, and the ectopic expression of Twist conferred resistance to microtubule-disrupting agents, including paclitaxel (27). Although details of the relevant mechanisms are still under investigation, it is possible that the increased expression of Twist is involved in the mechanisms underlying the occurrence of EMT in DDP-resistant cells.

To our knowledge, chemotherapeutic agents, including DDP, generally induce tumor regression through apoptosis, which is modulated through a series of proto-oncogenes and tumor suppressor genes (28,29). However, alterations in the regulation of such apoptotic processes may lead to increased expression levels of EMT-related molecules and result in the failure of therapy. Although the mechanisms underlying resistance to DDP and EMT are still under investigation (30), we argue that our finding that DDP-resistant NPC cells undergo EMT reflects an important process by which cancer cells may potentially acquire chemoresistance. Blocking or reversing EMT changes may cause chemoresistant cells to revert to chemosensitive cells.

In conclusion, we demonstrate that the development of resistance to DDP in NPC cells is accompanied by inducible EMT-like changes with an increased metastatic potential *in vitro*. Further elucidation of the association between resistance to DDP and EMT would allow the development of novel therapeutic approaches for chemoresistant tumors in the future.

Acknowledgements

The present study was supported by grants from the National Natural Science Foundation of China (81372899, 81072207), the Natural Science Foundation of Anhui Province (090413135) and the Key Project of Natural Science Research of the Education Department of Anhui Province, China (KJ2012A202), the innovation project of graduate scientific research of Bengbu Medical College of Anhui Province, China (Byycx1327).

References

1. Jemal A, Bray F, Center MM, Ferlay J, Ward E and Forman D: Global cancer statistics. CA Cancer J Clin 61: 69-90, 2011.
2. Chen QY, Wen YF, Guo L, *et al*: Concurrent chemoradiotherapy vs radiotherapy alone in stage II nasopharyngeal carcinoma: phase III randomized trial. J Natl Cancer Inst 103: 1761-1770, 2011.
3. Brabec V and Kasparkova J: Modifications of DNA by platinum complexes. Relation to resistance of tumors to platinum antitumor drugs. Drug Resist Updat 8: 131-146, 2005.
4. Li Q, Kawamura K, Yamanaka M, *et al*: Upregulated p53 expression activates apoptotic pathways in wild-type p53-bearing mesothelioma and enhances cytotoxicity of cisplatin and pemetrexed. Cancer Gene Ther 19: 218-228, 2012.
5. Wang L, Xiang S, Williams KA, *et al*: Depletion of HDAC6 enhances cisplatin-induced DNA damage and apoptosis in non-small cell lung cancer cells. PLoS One 7: e44265, 2012.
6. Shellard SA, Fichtinger-Schepman AM, Lazo JS and Hill BT: Evidence of differential cisplatin-DNA adduct formation, removal and tolerance of DNA damage in three human lung carcinoma cell lines. Anticancer Drugs 4: 491-500, 1993.
7. Torigoe T, Izumi H, Ishiguchi H, *et al*: Cisplatin resistance and transcription factors. Curr Med Chem Anticancer Agents 5: 15-27, 2005.
8. Cheung HW, Jin DY, Ling MT, *et al*: Mitotic arrest deficient 2 expression induces chemosensitization to a DNA-damaging agent, cisplatin, in nasopharyngeal carcinoma cells. Cancer Res 65: 1450-1458, 2005.

9. Hugo H, Ackland ML, Blick T, *et al*: Epithelial - mesenchymal and mesenchymal - epithelial transitions in carcinoma progression. J Cell Physiol 213: 374-383, 2007.
10. Thiery JP and Sleeman JP: Complex networks orchestrate epithelial-mesenchymal transitions. Nat Rev Mol Cell Biol 7: 131-142, 2006.
11. Kim MR, Choi HK, Cho KB, Kim HS and Kang KW: Involvement of Pin1 induction in epithelial-mesenchymal transition of tamoxifen-resistant breast cancer cells. Cancer Sci 100: 1834-1841, 2009.
12. Kajiyama H, Shibata K, Terauchi M, *et al*: Chemoresistance to paclitaxel induces epithelial-mesenchymal transition and enhances metastatic potential for epithelial ovarian carcinoma cells. Int J Oncol 31: 277-283, 2007.
13. Yang AD, Fan F, Camp ER, *et al*: Chronic oxaliplatin resistance induces epithelial-to-mesenchymal transition in colorectal cancer cell lines. Clin Cancer Res 12: 4147-4153, 2006.
14. Gu MF, Liu LZ, He LJ, *et al*: Sequential chemoradiotherapy with gemcitabine and cisplatin for locoregionally advanced nasopharyngeal carcinoma. Int J Cancer 132: 215-223, 2013.
15. Xie SM, Fang WY, Liu TF, Yao KT and Zhong XY: Association of ABCC2 and CDDP-resistance in two sublines resistant to CDDP derived from a human nasopharyngeal carcinoma cell line. J Oncol 2010: 915046, 2010.
16. Wong RS and Cheong SK: Leukaemic stem cells: drug resistance, metastasis and therapeutic implications. Malays J Pathol 34: 77-88, 2012.
17. Valastyan S and Weinberg RA: Tumor metastasis: molecular insights and evolving paradigms. Cell 147: 275-292, 2011.
18. Danila DC, Heller G, Gignac GA, *et al*: Circulating tumor cell number and prognosis in progressive castration-resistant prostate cancer. Clin Cancer Res 13: 7053-7058, 2007.
19. Liang Y, Meleady P, Cleary I, McDonnell S, Connolly L and Clynes M: Selection with melphalan or paclitaxel (Taxol) yields variants with different patterns of multidrug resistance, integrin expression and *in vitro* invasiveness. Eur J Cancer 37: 1041-1052, 2001.
20. Haga A, Nagase H, Kito H and Sato T: Invasive properties of cadmium-resistant human fibrosarcoma HT-1080 cells. Cancer Biochem Biophys 15: 275-284, 1997.
21. Wang Z, Li Y, Ahmad A, *et al*: Targeting miRNAs involved in cancer stem cell and EMT regulation: An emerging concept in overcoming drug resistance. Drug Resist Updat 13: 109-118, 2010.
22. Haslehurst AM, Koti M, Dharsee M, *et al*: EMT transcription factors snail and slug directly contribute to cisplatin resistance in ovarian cancer. BMC Cancer 12: 91, 2012.
23. Moustakas A and Heldin CH: Signaling networks guiding epithelial-mesenchymal transitions during embryogenesis and cancer progression. Cancer Sci 98: 1512-1520, 2007.
24. Pai MH, Kuo YH, Chiang EP and Tang FY: S-Allylcysteine inhibits tumour progression and the epithelial-mesenchymal transition in a mouse xenograft model of oral cancer. Br J Nutr 108: 28-38, 2012.
25. Jing Y, Han Z, Liu Y, *et al*: Mesenchymal stem cells in inflammation microenvironment accelerates hepatocellular carcinoma metastasis by inducing epithelial-mesenchymal transition. PLoS One 7: e43272, 2012.
26. Comijn J, Berx G, Vermassen P, *et al*: The two-handed E box binding zinc finger protein SIP1 downregulates E-cadherin and induces invasion. Mol Cell 7: 1267-1278, 2001.
27. Wang X, Ling MT, Guan XY, *et al*: Identification of a novel function of TWIST, a bHLH protein, in the development of acquired taxol resistance in human cancer cells. Oncogene 23: 474-482, 2004.
28. Rudin CM, Yang Z, Schumaker LM, *et al*: Inhibition of glutathione synthesis reverses Bcl-2-mediated cisplatin resistance. Cancer Res 63: 312-318, 2003.
29. Shen DW, Pouliot LM, Hall MD and Gottesman MM: Cisplatin resistance: a cellular self-defense mechanism resulting from multiple epigenetic and genetic changes. Pharmacol Rev 64: 706-721, 2012.
30. Barr MP, Gray SG, Hoffmann AC, *et al*: Generation and characterisation of cisplatin-resistant non-small cell lung cancer cell lines displaying a stem-like signature. PLoS One 8: e54193, 2013.